ACS APPLIED MATERIALS & INTERFACES

Research Article

Cite This: ACS Appl. Mater. Interfaces 2019, 11, 32390−32397

www.acsami.org

High-Performance Colorimetric Room-Temperature NO_2 Sensing Using Spin-Coated Graphene/Polyelectrolyte Reflecting Film

Hong Chi,*[,†] Zhen Xu,[†] Xiaosen Duan,[†] Jing Yang,[‡] Fuke Wang,[‡] and Zibiao Li*[,‡]

[†]Shandong Provincial Key Laboratory of Molecular Engineering, School of Chemistry and Pharmaceutical Engineering, Qilu University of Technology (Shandong Academy of Sciences), Jinan 250353, China

[‡]Institute of Materials Research and Engineering, A*STAR (Agency for Science, Technology and Research), 2 Fusionopolis Way, Innovis, #08-03, Singapore 138634, Singapore

Supporting Information

ABSTRACT: Nitrogen dioxide (NO_2) is a colorless, flammable, and dangerous gas even at very low concentrations. To date, quantitative analysis of NO_2 concentrations have been made using conventional techniques (e.g., electrochemical method). In light of the energy and time consumption involved in such applications, efforts have been made to develop new detection methods that are more sensitive and sustainable. At this point, structural color-based sensing shows great advantages because of its sensitive, visualized, and reproducible response. In this study, graphene oxide/polystyrene sulfonate (GO/PSS) optical films were designed and prepared to evaluate the potential usage for the effective detection of NO_2. The uniform GO/PSS thin films were fabricated by the spin-coating-assisted layer-by-layer assembly method. The resulting colorful films exhibited ultrafast response, obvious optical shifts, and good reversibility within the visible range toward NO_2. The concentration-dependent NO_2 sensing characteristics and selectivity were investigated as well. The dynamic study showed that the absorption/desorption time was 200/200 ms and the detection limit was 1.0 ppm at room temperature. The sensing mechanism was investigated and verified by computer simulations. Such ultrasensitive and colorimetric properties of GO/PSS films may enable many potential applications such as disposable sensors for health and environmental monitoring.

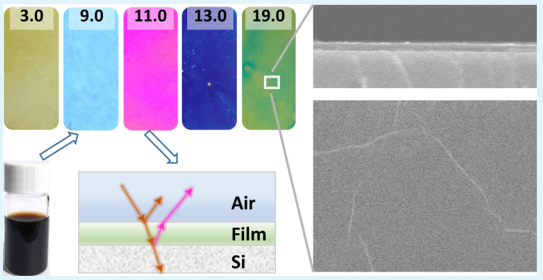

KEYWORDS: *graphene, structural color, NO_2 sensing, room temperature, layer-by-layer*

INTRODUCTION

Nitrogen dioxide (NO_2) is a colorless, flammable, and dangerous gas even at very low concentrations. NO_2 is formed via many pathways, such as car exhaust, burning of fossil fuels, and emissions from industrial production. As per the present Occupational Safety and Health Administration (OSHA) standards, the permissible exposure limit of NO_2 is 5 ppm. Besides, NO_2 detection is of paramount importance in warehouse for explosives as it is a decomposed product of many explosives. Hence, a sensitive and selective detection of NO_2 for real-time monitoring of its concentration is of great importance from the environmental protection and public health points of view. Over the past few decades, various reliable NO_2 gas sensors have already been developed. The materials reported for NO_2 detection mainly include metal oxide/metallic nanoparticles,[1−4] polymers,[5,6] and carbon hybrids.[7,8] However, most current gas sensors need to be operated either at elevated temperatures or based on electrochemical signal outputs which definitely increase the power consumption, shortening the on-shelf lifetime and increased risk in explosive detection.[9−11]

Structural color displaying materials have shown advantages and importance in the development of dynamic data display.[12] Recently, thin-film interference structural colors, because of the characteristics of simple material preparation, stable physical color, energy-saving, and environmental protection, have gradually attracted people's attention. When the incident light is reflected at different interfaces, the reflected light from the different upper and lower surfaces exhibits visualized color because of the interference overlap of different optical paths and phases.

Graphene is a perfect candidate for structural color-based optical gas sensing. The ultrathin two-dimensional (2D) monolayer structure would facilitate a more precise study of the effect of layer spacing on structural colors. Theoretically, the large specific surface area (theoretical value of 2630 m^2/g)[13] would enable the sensing of trace amounts of analytes. Moreover, graphene shows femtosecond optical response characteristics, and only 2.3% absorption of light, which can reflect visible light efficiently. Therefore, we would propose to develop an optical gas sensing platform based on the interference light changes of graphene oxide (GO) thin films. Even though we have reported the optical sensing of GO thin films for humidity and ethyl alcohol sensing,[14,15] they all

Received: June 10, 2019
Accepted: August 8, 2019
Published: August 8, 2019

DOI: 10.1021/acsami.9b09901
ACS Appl. Mater. Interfaces 2019, 11, 32390−32397

displayed interference toward NO_2 detection. Furthermore, the reported graphene-based gas sensors are normally easy to suffer from aggregation and poor selectivity. To create more active centers for NO_2 adsorption, various sulfonic acids such as dodecyl benzene sulfonic acid (DBSA), camphor sulfonic acid, b-naphthalene sulfonic acid, DBSA, and *p*-toluenesulfonic acid have been explored as dopants.[16−19] As a typical anionic polyelectrolyte, polystyrene sulfonate (PSS) offers benzene rings as the driving force for $\pi-\pi$ stacking with graphene and sulfophenyl groups for compelling to reduce the aggregation of graphene. Therefore, PSS was used to increase the dispersibility, selectivity of graphene sensing toward NO_2 because of the functional tunability, easy processing, and porosity of polymer materials.[20]

To study the influence of NO_2 on the interference light change, the film should be uniform and the thickness should be accurately controllable. Compared with the traditional film-forming methods such as drop coating and vacuum-assisted filtration, sputter deposition is a versatile technique for controlling the optical properties of the respective physical colors of thin films for various applications by modifying their composition and manipulating the arrangement of atoms without chemical synthesis and purification.[21] Layer-by-layer (LbL) assembly exhibited its strength in reducing micropleats and thickness control when preparing graphene films.[22,23] Graphene/quantum dot photocatalytic composite films have been prepared by this method, which can effectively adjust the film thickness and structure.[24] Su et al. used electrostatic interaction to assemble a polyelectrolyte/graphene lithium−sulfur battery material to obtain a very stable thin-film coating.[25] Spin coating is an efficient method in creating large-scale polymer films. The residual film thickness can be controlled via spinning velocity, concentration, molar mass, and molar mass distribution.[26] The Caruso team recently reviewed the spin-coating-assisted layer self-assembly method (SA-LbL) in controlling the surface roughness and ordered assembly of materials.[27] SA-LbL is beneficial to improve assembly efficiency, generate strong centripetal force and shear stress during high-speed rotation, help to open sheet material, prevent stacking and wrinkles, and form a smooth assembly surface, uniform topography and high surface coverage.[27,28]

Herein, uniform GO/PSS thin films for optical gas sensing were fabricated by the SA-LbL method. The resulted colorful GO/PSS thin films exhibited ultrafast response, good reversibility, and obvious optical shifts within the visible range toward NO_2. Dynamic study showed that the absorption time was 200 ms and the detection limit was 1.0 ppm. The selectivity of the GO/PSS sensor was studied by measuring the optical shifts toward various gases and vapors, including NO_2, ethyl alcohol, ammonia, formaldehyde, tetrahydrofuran, humidity, hydrogen sulfide, acetonitrile, sulfur dioxide, toluene, carbon monoxide, ethyl ether, dichloromethane, ethyl acetate, hexane, chloroform, and dimethyl sulfoxide. The sensing mechanism was investigated and verified via computer simulations.

EXPERIMENTAL SECTION

Materials. Commercially available GO solutions (~2 μm, 12.0 mg/mL) were supplied by Carmery (Institute of Coal Chemistry, Chinese Academy of Sciences). Poly(styrene sulfonic acid) sodium salt (PSS) with M_w 70 000 was purchased from Alfa Aesar. Silicon wafers [p-doping (100)] were purchased from Zhejianglijing Technology Co., Ltd. Ultrapure water (18.2 MΩ·cm at 25 °C) was collected from a Milli-Q integral water purification system. All chemicals obtained were used directly without further purification. GO was diluted to 1.5 mg/mL in an aqueous solution. PSS was dissolved in water and stirred overnight to prepare a homogeneous solution with a concentration of 8 mg/mL. Both solutions contained NaCl with a concentration of 1.0 M. The silicon wafers or quartz slides were treated with piranha solution [1:3 (v/v) mixture of 30% H_2O_2 and 98% H_2SO_4] to get a hydrophilic surface with Si−OH groups. Note that the piranha solution reacts violently with organic materials and should be handled carefully.

Instruments and Methods. The detailed characterization of instruments, device fabrication, and test conditions are exhibited in the Supporting Information.

Preparation of GO/PSS Films by Spin-Coating on Si Substrates. Initially, six layers of GO on a silicon wafer were spin-coated at 600 rpm for 20 s and then 1400 rpm for 50 s to increase the in-plane thickness of the GO/PSS films. This process was repeated for six times to get the precursor layer. After the GO layer dried in air, PSS was spin-coated on top of the GO layers at a spin rate of 2400 rpm to form one PSS layer. Subsequently, another single GO layer was coated at a spin rate of 1400 rpm. Finally, $(GO/PSS)_b$ films, with the number of bilayers denoted as *b*, were obtained by alternatively coating GO and PSS until a desired layer number was reached. Then, the film was allowed to be dried at room temperature before further usage. Finally, various colored and structural stable films can be obtained even after 1 year storage in atmosphere.

Gas Sensing Behavior. A piece of 2.0 cm × 2.0 cm GO/PSS film on a silicon wafer was placed into a 2.0 cm × 2.5 cm × 3.0 cm homemade quartz box. It was connected to a gas flow system including a nitrogen gas (N_2) cylinder and nitrogen dioxide (NO_2) cylinder or different organic solvents in the spectrometer chamber. A sealed three-necked round-bottom flask with various saturated salt solutions was used to provide different humidity environments. Several flow controllers were used to control and modulate the flow rate of the carrier gas (N_2) and the gas or vapor, as shown in Figure S1. The reflectance spectra of the GO/PSS film in different conditions were measured at the reflectance mode using a UV−vis spectrophotometer. The incident lights irradiated from the front side of the box only.

RESULTS AND DISCUSSION

Characterization. Graphite, GO, and GO/PSS were prepared by SA-LbL and were characterized by the Fourier transform infrared spectra (see Supporting Information, Figure S2). A broad peak that appeared from 3000 to 3600 cm^{-1} was assigned to the stretching and bending vibrations of −OH groups on GO. The presence of peaks at 1721, 1401, 1234, and 1058 cm^{-1} was ascribed to the stretching vibrations of −C═O, −C−O, C−O−C and -C-O, respectively, indicating the strong hydrophilic nature of GO. The asymmetric and symmetric vibrational peaks of the SO_3^- group can be found at 1185, 1120, and 1038 cm^{-1}, respectively. The peaks that appeared at 1550, 1450, and 1410 cm^{-1} were assigned to the stretching vibration of the C═C bond with S in benzene rings. The appearance of each characteristic peak in the GO/PSS film suggested the successful coating of each layer.

The surface morphology of GO/PSS was investigated by scanning electron microscopy (SEM). Although spin-coating can be used to improve assembly efficiency, generate strong centripetal force and shear stress during high-speed rotation which might be helpful to open sheet material, and prevent stacking and wrinkling, a few wrinkles still could be observed from the flat and homogeneous surface (Figure 1A). This is probably because of the Brownian motion and capillary forces that resulted in folding in the drying process;[29,30] however, the cross-sectional image of $(GO/PSS)_3$ in Figure 1B indicated that the thickness of the film was not affected by wrinkles.

DOI: 10.1021/acsami.9b09901
ACS Appl. Mater. Interfaces 2019, 11, 32390−32397

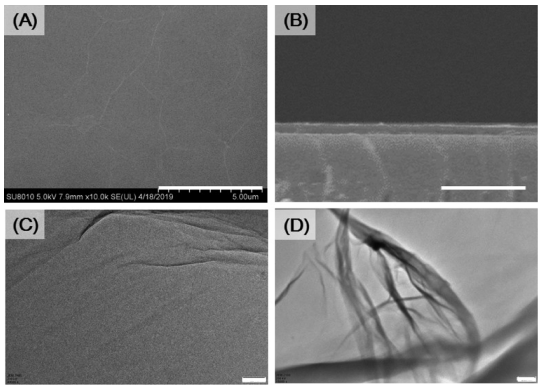

Figure 1. SEM (A,B) characterization of the spin-coated $(GO/PSS)_9$ film (scale bar indicated 5 and 1 μm, respectively) and TEM (C,D) characterization of the physically mixed GO/PSS (scale bar indicated 200 and 100 nm, respectively).

According to the principle of thin-film interference reported in our previous work,[15] the total light waves reflected by certain coating depend on the relative coating thickness, and the thicker the GO film, the longer the wavelength is. It was also testified that the GO wrinkles did not show an optical loss range from 200 to 800 nm. To verify that no agglomerates were formed between GO and PSS, transmission electron microscopy (TEM) test was performed by physically mixing the same ratio of GO and PSS in water. Figure 1C,D revealed the well-dispersed GO in the mixture which further confirmed that the wrinkles were formed during spin-coating.

Visualized Color of GO/PSS Films. Figure 2A shows the photographs of the $(GO/PSS)_b$ films with b varying from 3.0 to 19.0, taken at a viewing angle of 90° to the film surface. The films exhibited highly distinguishable colors under ambient conditions with a relative humidity (RH) of ca. 52% and temperature of ca. 25 °C. Depending on the number of pairs, the films showed brownish yellow, light blue, purple, deep blue, and green color. Such homogeneous coating can be realized on silicon wafers with a diameter of 2.50 cm (Figure S3). The reflectance spectra of the film showed bathochromic shift proportional to b; however, the spectral and visualized color of GO/PSS became indistinguishable when b is less than or equal to 3. The position of the maximum reflected wavelength corresponds to the thickness of the films, with the sequence indicated by arrows. Although there is size distribution and wrinkles between the GO nanosheets (Figure S4), the visualized color and the reflectance spectra of the film were mainly determined by the statistical thickness, as demonstrated in our previous report.[14,15]

As illustrated in Figure 2B, when incident light irradiated the surface of the film, a part of light will be reflected by the surface, and the other part of light will either be transmitted or reflected by the lower boundaries.[31] Then, the second reflection and refraction at the interface will interfere with the first reflected light at the air-coating interface. Thus, the reflected intensity at a certain wavelength by the thin film will be increased or decreased because of the constructive or destructive light, depending on the thickness of the coating.[32] L represents the effective thickness and X is the displacement between the first reflected light and the second reflected light. The relation between the wavelength of incident light (λ) and the film thickness (h) of the GO/PSS coating can be expressed according to the principle of thin-film interference by eq 1

$$2nh\cos(\theta_r) = m\lambda \quad (1)$$

where n represents the refractive index of the GO/PSS film, θ_r is the angle of refraction, h is the film thickness, and m is an integer. According to eq 1, there should be an optimized film thickness to observe the color film in the visible light range from 400 to 700 nm. Therefore, films with several bright colors (Figure 2A) were prepared. The deep blue $(GO/PSS)_{13}$ with a thickness of 180 nm was used for gas sensing study because of the color distinguishable from the neighboring ones.

Colorimetric Sensing upon Exposure to NO_2 Gas Atmosphere. To evaluate the sensing performance of GO/PSS toward NO_2, the reflectance spectra of $(GO/PSS)_{13}$ in different concentrations of NO_2 gas were collected, with the detection angle perpendicular to the incident light. The different concentrations of NO_2 were obtained by diluting the standard gas with different volumes of dry nitrogen. A commercial gas sensor based on an electrochemical method was used to further verify each targeted concentration. Figure 3A suggested that the detection of 5 ppm NO_2 was not affected by ambient RH obviously.

The film response to the different concentrations of NO_2 affected by humidity was verified by both spectral shifts and color change, as shown in Figure 3B–D. At ambient humidity (52% RH), $(GO/PSS)_{13}$ exhibited a 35 nm blue shift as the gas concentration increased from 0 to 100 ppm. The blue shift was even larger (50 nm) at higher humidity. The results indicated that water molecules may facilitate the intercalation of NO_2 into the interlayers of GO/PSS. This is quite interesting because normally the gas sensing of graphene derivatives is based on the gas intercalation, followed by an increase in the

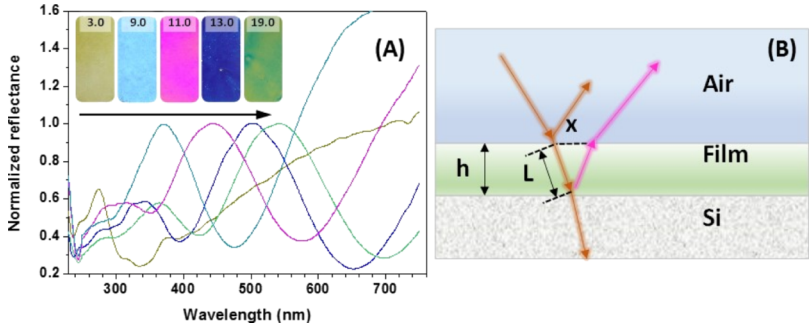

Figure 2. (A) UV–vis reflecting spectral shifts of the GO/PSS film with bright color by tuning the number of pairs (b = 3.0, 9.0, 11.0, 13.0, and 19.0) of GO/PSS. (B) Schematic illustration of the thin-film interference across GO/PSS.

DOI: 10.1021/acsami.9b09901
ACS Appl. Mater. Interfaces 2019, 11, 32390–32397

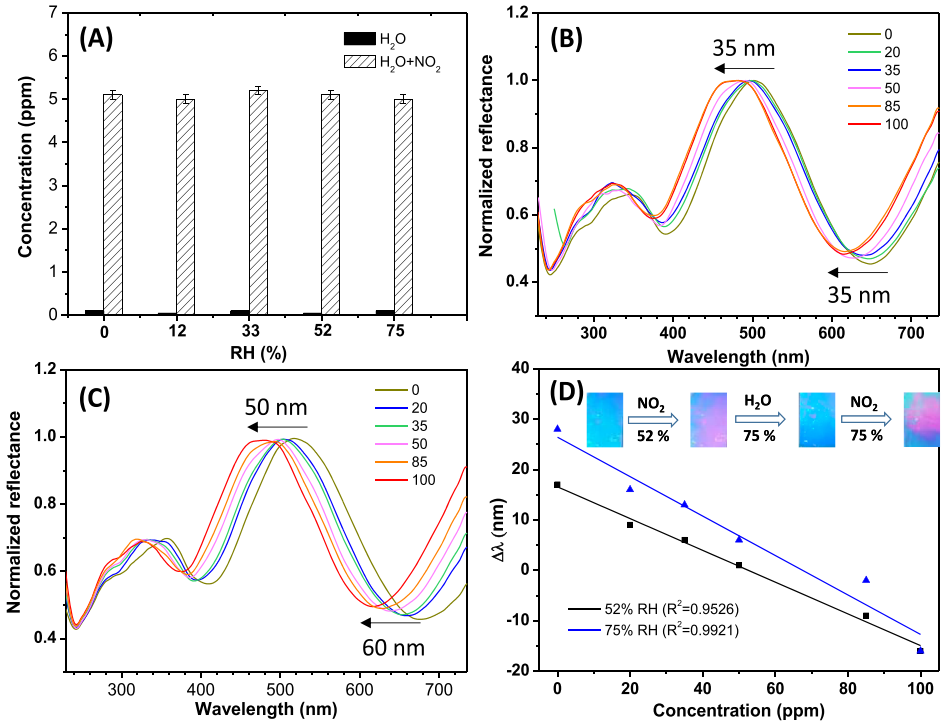

Figure 3. (A) NO_2 (5 ppm) at different RH % tested by a commercial gas monitor. (B) Wavelength shift of $(GO/PSS)_{13}$ when exposed to different concentrations of NO_2 in 52% RH and (C) 75% RH. (D) Linear relation between the wavelength shift and the concentration of NO_2 when exposed to 52 and 75% RH atmosphere. The inset image shows the color evolution of the $(GO/PSS)_{13}$ film. The concentration of NO_2 is 2.1 ppm.

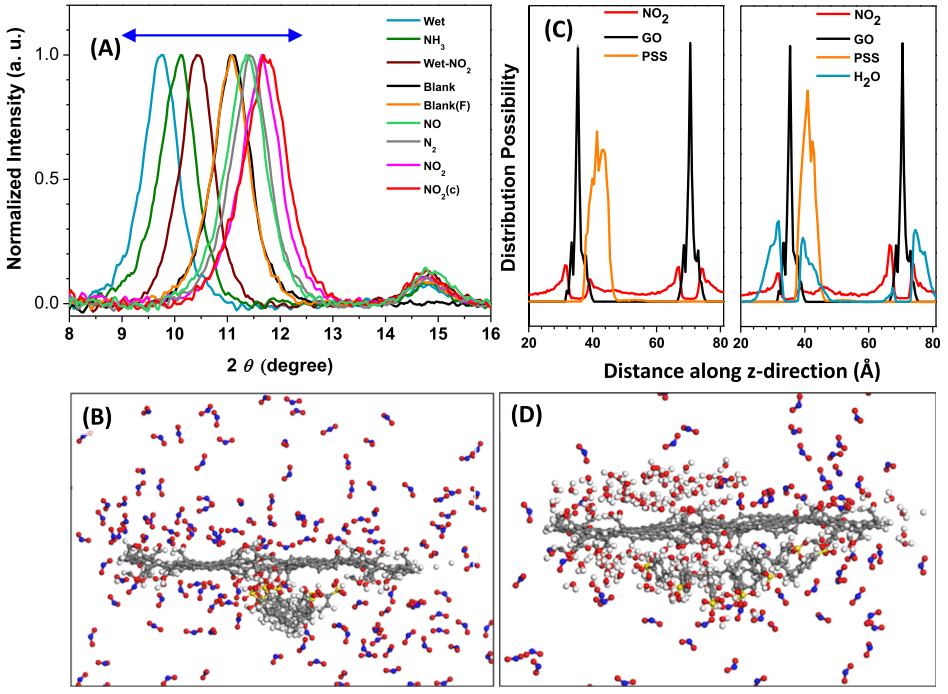

Figure 4. (A) XRD of $(GO/PSS)_{13}$ exposed to (from left to right) 75% RH (wet), 100 ppm dry NH_3 (NH_3), 100 ppm NO_2 in 75% RH (wet NO_2), 52% RH without parafilm (Blank), 52% RH [Blank (F)], concentrated dry NO (NO), dry N_2 (N_2), 100 ppm dry NO_2 (NO_2), and concentrated dry NO_2 [NO_2 (c)]. All the tested atmospheres were sealed with parafilm (F) except the blank sample. (B) Simulated molecular absorption of NO_2 on assembled GO/PSS. (C) Simulated molecular absorption of NO_2 with H_2O. (D) Calculated number of molecules intercalated in between layers. C, O, N, S, and O on NO_2 were indicated by gray, white, blue, yellow, and red colors, respectively.

film thickness. Previous studies also revealed that the hydrophilic surface of GO could provide a favorable environment for the intercalation of H_2O,[14,33,34] O_2,[35] and CO_2.[36] It can be deduced that there is a synergistic intercalation effect between water and NO_2 in the GO/PSS film. The plots in Figure 3D displayed the relation between the wavelength shift and the concentration of NO_2 at 52 and 75% RH extracted from Figure 3B,C. The good linear relation in between

DOI: 10.1021/acsami.9b09901
ACS Appl. Mater. Interfaces 2019, 11, 32390−32397

Table 1. Performance of the Sensor in This Work Compared with Previous Works

sensor type	material	detection range (ppm)	exposure time (min)	working temperature (°C)	response/recovery time (s)	references
resistance	In_2O_3	1−50		250	5/14	38
resistance	SnO_2/SnS_2	1−8		80	159/297	2
resistance	SnO_2/rGO	2−110		55	373	39
resistance	GO/α-Fe_2O_3	0.1−5.0		25	32/1435	40
resistance	rGO	1−20	20		420/1680	41
conductance	rGO-Cu_2O	0.4−2.0		25	250/500	42
conductance	phosphorene	0.02−1.0		25	∼600/480	43
structural color	GO/PSS	1−100		25	0.2/0.2	this work

suggests the promising sensing of NO_2 by the colorimetric method. The visualized detection limit is 1 ppm, as observed from 30° to the film in ambient environment, as shown in Video S1. The screenshot from the Videos S1 and S2 in Figure 3D shows that $(GO/PSS)_{13}$ was quite sensitive to NO_2 but insensitive to water intercalation when RH rose from 52 to 75%.

Mechanism of Sensing. To confirm gas intercalation, X-ray diffraction (XRD) of $(GO/PSS)_{13}$ in different atmospheres sealed by parafilm was carried out. As shown in Figure 4A, the peaks of the parafilm appeared at 6.55°, 14.8°, 21.4°, and 23.9°, and it does not affect the diffraction of GO/PSS. Thus, the peak at 14.8° was selected as an internal standard for the comparison of peak shifts. The (002) diffraction peak of GO in 52% RH appeared at 11.09°, which corresponds to a layer distance of 0.797 nm. Upon exposure to NO_2 in 75% RH, 100 ppm dry NH_3, or 75% RH, this peak shifted to 10.43°, 10.12°, and 9.76°, respectively. According to Bragg's law, these shifts indicated the intercalation and expansion of the GO layers.

Interestingly, when the film was exposed to 100 ppm dry NO_2, the peak shifted to 11.65°, revealing that GO/PSS was heavily contracted in the NO_2 atmosphere and the layer distance reduced to 0.759 nm. Higher concentration of dry NO_2 resulted in a more obvious contraction effect. To eliminate the effect of NO that might be generated between the reaction of NO_2 and H_2O, a high concentration of NO was also tested. The results indicated that NO could also cause the contraction effect, but it is possibly because of the drying effect, on further comparison with dry N_2. During the experiment, the color change of the film was stable in half an hour.

This is in excellent agreement with our assumption. In the GO/PSS thin film, PSS contained the negatively charged sulfonate group and GO was enriched with the negatively charged carboxylic group. Upon exposure, the electron-deficient NO_2 would anchor to the electron-rich site, namely the atoms with lone-pair electrons or the negative charges. Leenaerts et al. performed a first-principles study of the gas adsorption ability on graphene. According to their conclusion, paramagnetic molecules such as NO_2 could interact with graphene as an electron acceptor, whereas NH_3, CO, H_2S, acetone, ethanol, and so forth could work as electron donors.[37] Kim and co-workers investigated gas intercalation in both dry and moisture-swelled GO interlayers. It was found that only hydrophilic gases can be intercalated into dried GO. However, all the tested CO_2, CH_4, N_2, and H_2 exhibited intercalation into water-swelled GO because of the affinity among the gas, water molecules, and functional groups on the GO plane. From the molecular dynamics simulations, it was found that CO_2 molecules were mainly solvated by water molecules and located in the middle of the interlayer.[36] Therefore, GO may work as a p-type semiconductor for the intercalation of water molecules, resulting in the increase of interlayer distances. After this, the hydrophilic NO_2 could enter into the negatively charged GO/PSS layers and work as an electron acceptor, leading to a decrease in the film thickness. This is also consistent with the experimental result that we could not observe a color change in the thinnest $(GO/PSS)_3$ film, as shown in Video S3. To further confirm the sensing mechanism, computer simulations were performed. As shown in Figure 4B, the NO_2 molecules homogeneously distributed around the GO plane, which was further revealed by the molecule distribution in Figure 4C. With the addition of H_2O, the sulfonate group of PSS inverted to the outside and NO_2 molecules were mostly located in the GO side. The absorbed water molecules formed a cage-like structure, providing hydrogen-bonding networks near the PSS side, as shown in Figure 4C,D.

Sensing Performance. Table 1 presents the NO_2 sensing characteristics of the proposed GO/PSS sensor in comparison with previous works. The measurement range for the prepared film is comparable to those materials made of metal oxides and GO-based hybrids and sensing types of resistance and conductance. As shown in Table 1, earlier research represented by In_2O_3 and SnO_2/SnS_2 showed a modest sensitivity and response time toward the ppm-level NO_2 gas below 80 °C. Additionally, novel 2D materials such as graphene derivatives and phosphorene are emerging and exhibiting good sensitivity toward NO_2 detection at room temperature. Comparatively, the colorimetric GO/PSS sensing film showed an ultrafast response at room temperature so as to meet the requirements of trace detection in the range of 1−100 ppm. The sensing selectivity of GO/PSS was also studied upon exposure to various gases and vapors, including NO_2, ethyl alcohol, ammonia, formaldehyde, tetrahydrofuran, humidity, hydrogen sulfide, acetonitrile, sulfur dioxide, toluene, carbon monoxide, ethyl ether, dichloromethane, ethyl acetate, hexane, chloroform, and dimethyl sulfoxide. As shown in Figure 5, the film exhibited the opposite and strongest optical shift toward NO_2 among all tested analytes, indicating the high sensing selectivity for NO_2 detection.

According to the mechanism of response, a gas can be detected only when it can intercalate into the anion oxygen-enriched GO−PSS layers at a certain humidity. Therefore, the physical properties and optical shifts of organic vapors are summarized and shown in Table S1 and Figure S5. Vapor with low polarity such as hexane, toluene, dichloromethane, chloroform, ethyl ether, and carbon monoxide exhibited a low optical shift because of the mismatch of polarity with GO/PSS. Large gas molecules such as sulfur dioxide and dimethyl sulfoxide also showed a low shift value. Tetrahydrofuran, acetonitrile, and dimethyl sulfoxide are vapors of high polarity, but dimethyl sulfoxide is a solvent with high boiling point and low vapor pressure.. Computer simulations (Supporting

DOI: 10.1021/acsami.9b09901
ACS Appl. Mater. Interfaces 2019, 11, 32390−32397

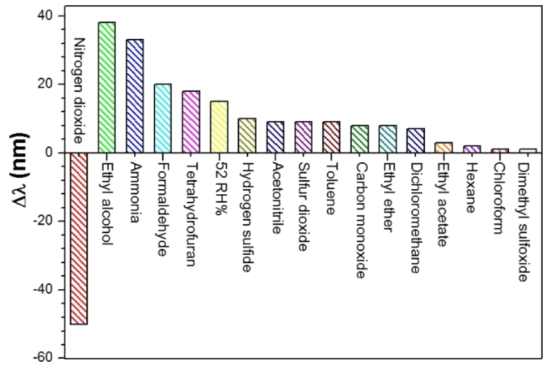

Figure 5. Detection selectivity of $(GO/PSS)_{13}$ upon exposure to various vapors (~100 ppm), operated at room temperature and 75% RH.

Information) indicated that the gas diffusion rate and adsorption energy of tetrahydrofuran and acetonitrile were much lower than that of NO_2. More studies on the sensing selectivity of graphene hybrids are currently underway, and a deep understanding of the selectivity is still needed.

Reversible Conversion of the GO Sensor. Figure 6 shows the dynamic response of the NO_2 gas sensor. The

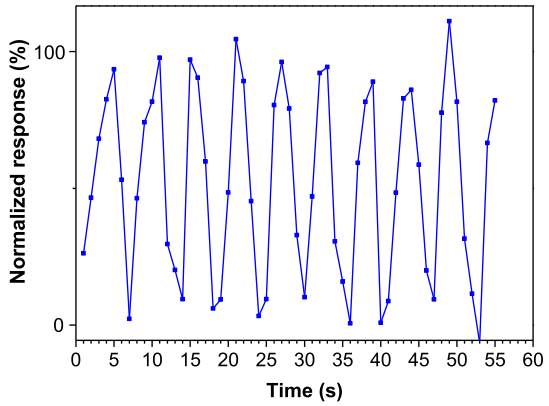

Figure 6. Response and recovery properties of the GO/PSS film upon exposure to 100 ppm NO_2 and RH of 75% at 25 °C.

reflectance wavelength at 505 nm was used for tracking. The gas response is calculated as the wavelength shift of the sensor in a specific atmosphere to the reflectance in dry nitrogen (response = $\Delta\lambda/\lambda$).

The response time here is defined as the time of the sensor exposure to the given concentration of gas. The recovery time is defined as the time of the sensor purged with dry nitrogen gas. Both the times include the gas diffusion and data collection times in the setups and instruments. As indicated in the figure, the average response and recovery times of the GO/PSS gas sensor herein were 1.8 and 2.5 s, respectively.

To reveal the real response time without gas diffusion and data collection times, Video S1 showed the response/recovery times of 200 ms/200 ms in ambient conditions. The stability of color change was verified by sealing the saturated salt solution (52% RH), 5 ppm NO_2, commercial gas sensor, and the GO/PSS film in a test box. The results revealed that the concentration of gas and the color of GO/PSS were stable in half an hour. Such ultrafast response/recovery times could be attributed to the abundant hydrophilic groups and porosity in 2D GO/PSS. The spectral shift of the GO/PSS film is completely reversible when the gas atmosphere is alternated between NO_2 and dry nitrogen, as evidenced by the test for 10 times. The deviations between each cycle can be ascribed to the structural rearrangement of the film between continuous contraction and swelling by gas absorption and desorption.

CONCLUSIONS

In this study, an ultrasensitive NO_2 sensor with the GO/polymer film was fabricated by using SA-LbL. GO/PSS were alternatively deposited on the silicon wafer substrate to form distinguishable color thin films. The thickness could be controlled by varying the number of layers. The gas sensing properties were investigated with varying gases at room temperature, revealing the visualized response−recovery within ca. 200 ms, characteristic with an outstanding stability and linearity. The possible mechanism for NO_2 sensing is the intercalation of water molecule-facilitated interaction. Water molecules may first increase the interlayer distance of GOs. After this, NO_2 could enter into the negatively charged GO/PSS layers and work as an electron acceptor, leading to a decrease in the film thickness and blue shift of the reflectance spectra. The novel gas sensor exhibited satisfactory sensing performance in the detection of NO_2 gas and can be practically used because of the ease and low cost of fabrication.

ASSOCIATED CONTENT

Supporting Information

The Supporting Information is available free of charge on the ACS Publications website at DOI: 10.1021/acsami.9b09901.

Schematic illustration of the gas dilution, sensing, and reflectometric test system; FTIR spectra of graphite, GO, and PSS and the GO/PSS film that scraped off; optical image of the spin-coated $(GO/PSS)_9$ on silicon wafer used for NO_2 sensing; surface view of the $(GO/PSS)_9$ thin film under an atomic force microscope; summarized physical properties of VOCs studied in gas selectivity; and reflectance spectra and molecular structure of the tested VOCs (PDF)

Visualized color change when exposed to NO_2 in 52% RH atmosphere (AVI)

Visualized color change when exposed to 75% RH atmosphere only (AVI)

Absence of color change in the thinnest $(GO/PSS)_3$ film (AVI)

AUTHOR INFORMATION

Corresponding Authors

*E-mail: ch9161@gmail.com. Phone: +86-13553197297 (H.C.).

*E-mail: lizb@imre.a-star.edu.sg. Phone: +65-63194767 (Z.L.).

ORCID

Jing Yang: 0000-0001-5851-2816

Fuke Wang: 0000-0002-6980-5857

Zibiao Li: 0000-0002-0591-5328

Notes

The authors declare no competing financial interest.

ACKNOWLEDGMENTS

This work was financially supported by the National Natural Science Foundation of China (grant no. 51702178), National

DOI: 10.1021/acsami.9b09901
ACS Appl. Mater. Interfaces 2019, 11, 32390−32397

Science Foundation of Shandong Province (grant nos. ZR2017QB003, ZR2018MB017), and Program for Scientific Research Innovation Team in Colleges and Universities of Shandong Province. The authors also express their gratitude to the A*STAR Research Grant for support of this project.

REFERENCES

(1) Wang, Y.; Cui, X.; Yang, Q.; Liu, J.; Gao, Y.; Sun, P.; Lu, G. Preparation of Ag-loaded Mesoporous WO_3 and Its Enhanced NO_2 Sensing Performance. *Sens. Actuators, B* **2016**, *225*, 544−552.
(2) Gu, D.; Li, X.; Zhao, Y.; Wang, J. Enhanced NO_2 Sensing of SnO_2/SnS_2 Heterojunction Based Sensor. *Sens. Actuators, B* **2017**, *244*, 67−76.
(3) Dai, Z.; Dai, H.; Zhou, Y.; Liu, D.; Duan, G.; Cai, W.; Li, Y. Monodispersed Nb_2O_5 Microspheres: Facile Synthesis, Air/Water Interfacial SelfAssembly, Nb_2O_5-Based Composite Films, and Their Selective NO_2 Sensing. *Adv. Mater. Interfaces* **2015**, *2*, 1500167.
(4) Zhang, J.; Liu, X.; Neri, G.; Pinna, N. Nanostructured Materials for Room-Temperature Gas Sensors. *Adv. Mater.* **2016**, *28*, 795−831.
(5) Pandey, S. Highly Sensitive and Selective Chemiresistor Gas/Vapor Sensors Based on Polyaniline Nanocomposite: A Comprehensive Review. *J. Sci.: Adv. Mater. Dev.* **2016**, *1*, 431−453.
(6) Zang, Y.; Huang, D.; Di, C.-a.; Zhu, D. Device Engineered Organic Transistors for Flexible Sensing Applications. *Adv. Mater.* **2016**, *28*, 4549−4555.
(7) Bai, S.; Guo, J.; Sun, J.; Tang, P.; Chen, A.; Luo, R.; Li, D. Enhancement of NO_2-Sensing Performance at Room Temperature by Graphene-Modified Polythiophene. *Ind. Eng. Chem. Res.* **2016**, *55*, 5788−5794.
(8) Wu, J.; Li, Z.; Xie, X.; Tao, K.; Liu, C.; Khor, K. A.; Miao, J.; Norford, L. K. 3D Superhydrophobic Reduced Graphene Oxide for Activated NO_2 Sensing with Enhanced Immunity to Humidity. *J. Mater. Chem. A* **2018**, *6*, 478−488.
(9) Zhang, K.; Zhou, H.; Mei, Q.; Wang, S.; Guan, G.; Liu, R.; Zhang, J.; Zhang, Z. Instant Visual Detection of Trinitrotoluene Particulates on Various Surfaces by Ratiometric Fluorescence of Dual-Emission Quantum Dots Hybrid. *J. Am. Chem. Soc.* **2011**, *133*, 8424−8427.
(10) Ou, P.; Zhang, R.; Liu, Z.; Tian, X.; Han, G.; Liu, B.; Hu, Z.; Zhang, Z. Gasotransmitter Regulation of Phosphatase Activity in Live Cells Studied by Three-Channel Imaging Correlation. *Angew. Chem., Int. Ed.* **2019**, *58*, 2261−2265.
(11) Zhang, R.; Zhao, J.; Han, G.; Liu, Z.; Liu, C.; Zhang, C.; Liu, B.; Jiang, C.; Liu, R.; Zhao, T.; Han, M.-Y.; Zhang, Z. Real-Time Discrimination and Versatile Profiling of Spontaneous Reactive Oxygen Species in Living Organisms with a Single Fluorescent Probe. *J. Am. Chem. Soc.* **2016**, *138*, 3769−3778.
(12) Arsenault, A. C.; Puzzo, D. P.; Manners, I.; Ozin, G. A. Photonic-Crystal Full-Colour Displays. *Nat. Photonics* **2007**, *1*, 468−472.
(13) Peigney, A.; Laurent, C.; Flahaut, E.; Bacsa, R. R.; Rousset, A. Specific Surface Area of Carbon Nanotubes and Bundles of Carbon Nanotubes. *Carbon* **2001**, *39*, 507−514.
(14) Chi, H.; Liu, Y. J.; Wang, F.; He, C. Highly Sensitive and Fast Response Colorimetric Humidity Sensors Based on Graphene Oxides Film. *ACS Appl. Mater. Interfaces* **2015**, *7*, 19882−19886.
(15) Gong, T.; Zhang, X.; Fu, Y.; Zhou, G.; Chi, H.; Li, T. A Facile Fabrication of Colorimetric Graphene Oxide Reflecting Films for Ultrasensitive Optical Gas Sensing. *Sens. Actuators, B* **2018**, *261*, 83−90.
(16) Mane, A. T.; Navale, S. T.; Patil, V. B. Room Temperature NO_2 Gas Sensing Properties of DBSA Doped PPy−WO_3 Hybrid Nanocomposite Sensor. *Org. Electron.* **2015**, *19*, 15−25.
(17) Basavaraja, C.; Kim, N.-R.; Jo, E.-A.; Pierson, R.; Huh, D.-S.; Venkataraman, A. Transport Properties of Polypyrrole Films Doped with Sulphonic Acids. *Bull. Korean Chem. Soc.* **2009**, *30*, 2701−2706.
(18) Navale, S. T.; Khuspe, G. D.; Chougule, M. A.; Patil, V. B. Camphor Sulfonic Acid Doped PPy/α-Fe_2O_3 Hybrid Nanocomposites as NO_2 Sensors. *RSC Adv.* **2014**, *4*, 27998−28004.
(19) Paul, S.; Joseph, M. Polypyrrole Functionalized with FePcTSA for NO_2 Sensor Application. *Sens. Actuators, B* **2009**, *140*, 439−444.
(20) Ogieglo, W.; Wormeester, H.; Eichhorn, K.-J.; Wessling, M.; Benes, N. E. In situ Ellipsometry Studies on Swelling of Thin Polymer Films: A review. *Prog. Polym. Sci.* **2015**, *42*, 42−78.
(21) Schwartzkopf, M.; Santoro, G.; Brett, C. J.; Rothkirch, A.; Polonskyi, O.; Hinz, A.; Metwalli, E.; Yao, Y.; Strunskus, T.; Faupel, F.; Müller-Buschbaum, P.; Roth, S. V. Real-time Monitoring of Morphology and Optical Properties During Sputter Deposition for Tailoring Metal−Polymer Interfaces. *ACS Appl. Mater. Interfaces* **2015**, *7*, 13547−13556.
(22) Vikulov, S.; Di Stasio, F.; Ceseracciu, L.; Saldanha, P. L.; Scarpellini, A.; Dang, Z.; Krahne, R.; Manna, L.; Lesnyak, V. Fully Solution-Processed Conductive Films Based on Colloidal Copper Selenide Nanosheets for Flexible Electronics. *Adv. Funct. Mater.* **2016**, *26*, 3670−3677.
(23) Mangadlao, J. D.; Santos, C. M.; Felipe, M. J. L.; de Leon, A. C. C.; Rodrigues, D. F.; Advincula, R. C. On the Antibacterial Mechanism of Graphene Oxide (GO) Langmuir−Blodgett Films. *Chem. Commun.* **2015**, *51*, 2886−2889.
(24) Xiao, F.-X.; Miao, J.; Liu, B. Layer-by-Layer Self-Assembly of CdS Quantum Dots/Graphene Nanosheets Hybrid Films for Photoelectrochemical and Photocatalytic Applications. *J. Am. Chem. Soc.* **2014**, *136*, 1559−1569.
(25) Wu, F.; Li, J.; Su, Y.; Wang, J.; Yang, W.; Li, N.; Chen, L.; Chen, S.; Chen, R.; Bao, L. Layer-by-Layer Assembled Architecture of Polyelectrolyte Multilayers and Graphene Sheets on Hollow Carbon Spheres/Sulfur Composite for High-Performance Lithium−Sulfur Batteries. *Nano Lett.* **2016**, *16*, 5488−5494.
(26) Schubert, D. W.; Dunkel, T. Spin Coating from a Molecular Point of View: Its Concentration Regimes, Influence of Molar Mass and Distribution. *Mater. Res. Innovations* **2003**, *7*, 314−321.
(27) Richardson, J. J.; Bjornmalm, M.; Caruso, F. Technology-Driven Layer-by-Layer Assembly of Nanofilms. *Science* **2015**, *348*, aaa2491.
(28) Chernikova, V.; Shekhah, O.; Eddaoudi, M. Advanced Fabrication Method for the Preparation of MOF Thin Films: Liquid-Phase Epitaxy Approach Meets Spin Coating Method. *ACS Appl. Mater. Interfaces* **2016**, *8*, 20459−20464.
(29) Nandy, K.; Palmeri, M. J.; Burke, C. M.; An, Z.; Nguyen, S. T.; Putz, K. W.; Brinson, L. C. Stop Motion Animation Reveals Formation Mechanism of Hierarchical Structure in Graphene Oxide Papers. *Adv. Mater. Interfaces* **2016**, *3*, 1500666.
(30) Zhang, M.; Wang, Y.; Huang, L.; Xu, Z.; Li, C.; Shi, G. Multifunctional Pristine Chemically Modified Graphene Films as Strong as Stainless Steel. *Adv. Mater.* **2015**, *27*, 6708−6713.
(31) Jung, I.; Rhyee, J.-S.; Son, J. Y.; Ruoff, R. S.; Rhee, K.-Y. Colors of Graphene and Graphene-Oxide Multilayers on Various Substrates. *Nanotechnology* **2011**, *23*, 025708.
(32) Xiao, M.; Li, Y.; Allen, M. C.; Deheyn, D. D.; Yue, X.; Zhao, J.; Gianneschi, N. C.; Shawkey, M. D.; Dhinojwala, A. Bio-Inspired Structural Colors Produced via Self-assembly of Synthetic Melanin Nanoparticles. *ACS Nano* **2015**, *9*, 5454−5460.
(33) Rezania, B.; Severin, N.; Talyzin, A. V.; Rabe, J. P. Hydration of Bilayered Graphene Oxide. *Nano Lett.* **2014**, *14*, 3993−3998.
(34) Wu, R.; Gan, L.; Ou, X.; Zhang, Q.; Luo, Z. Detaching Graphene from Copper Substrate by Oxidation-Assisted Water Intercalation. *Carbon* **2016**, *98*, 138−143.
(35) Grånäs, E.; Knudsen, J.; Schröder, U. A.; Gerber, T.; Busse, C.; Arman, M. A.; Schulte, K.; Andersen, J. N.; Michely, T. Oxygen Intercalation under Graphene on Ir (111): Energetics, Kinetics, and the Role of Graphene Edges. *ACS Nano* **2012**, *6*, 9951−9963.
(36) Kim, D.; Kim, D. W.; Lim, H.-K.; Jeon, J.; Kim, H.; Jung, H.-T.; Lee, H. Intercalation of Gas Molecules in Graphene Oxide Interlayer: The Role of Water. *J. Phys. Chem. C* **2014**, *118*, 11142−11148.

DOI: 10.1021/acsami.9b09901
ACS Appl. Mater. Interfaces 2019, 11, 32390−32397

(37) Leenaerts, O.; Partoens, B.; Peeters, F. M. Adsorption of H_2O, NH_3, CO, NO_2, and NO on Graphene: A First-Principles Study. *Phys. Rev. B: Condens. Matter Mater. Phys.* **2008**, *77*, 125416.
(38) Gao, L.; Cheng, Z.; Xiang, Q.; Zhang, Y.; Xu, J. Porous Corundum-Type In_2O_3 Nanosheets: Synthesis and NO_2 Sensing Properties. *Sens. Actuators, B* **2015**, *208*, 436−443.
(39) Li, L.; He, S.; Liu, M.; Zhang, C.; Chen, W. Three-Dimensional Mesoporous Graphene Aerogel-Supported SnO_2 Nanocrystals for High-Performance NO_2 Gas Sensing at Low Temperature. *Anal. Chem.* **2015**, *87*, 1638−1645.
(40) Zhang, H.; Yu, L.; Li, Q.; Du, Y.; Ruan, S. Reduced Graphene Oxide/α-Fe_2O_3 Hybrid Nanocomposites for Room Temperature NO_2 Sensing. *Sens. Actuators, B* **2017**, *241*, 109−115.
(41) Su, P.-G.; Shieh, H.-C. Flexible NO_2 Sensors Fabricated by Layer-by-Layer Covalent Anchoring and in Situ Reduction of Graphene Oxide. *Sens. Actuators, B* **2014**, *190*, 865−872.
(42) Deng, S.; Tjoa, V.; Fan, H. M.; Tan, H. R.; Sayle, D. C.; Olivo, M.; Mhaisalkar, S.; Wei, J.; Sow, C. H. Reduced Graphene Oxide Conjugated Cu_2O Nanowire Mesocrystals for High-Performance NO_2 Gas Sensor. *J. Am. Chem. Soc.* **2012**, *134*, 4905−4917.
(43) Cui, S.; Pu, H.; Wells, S. A.; Wen, Z.; Mao, S.; Chang, J.; Hersam, M. C.; Chen, J. Ultrahigh Sensitivity and Layer-Dependent Sensing Performance of Phosphorene-Based Gas Sensors. *Nat. Commun.* **2015**, *6*, 8632.

DOI: 10.1021/acsami.9b09901
ACS Appl. Mater. Interfaces 2019, 11, 32390−32397